Targeted degradation of sense and antisense *C9orf72* RNA foci as therapy for ALS and frontotemporal degeneration

Clotilde Lagier-Tourenne[a,b,1], Michael Baughn[a,1], Frank Rigo[c], Shuying Sun[b,d], Patrick Liu[d], Hai-Ri Li[d], Jie Jiang[b,d], Andrew T. Watt[c], Seung Chun[c], Melanie Katz[c], Jinsong Qiu[d], Ying Sun[a,b,d], Shuo-Chien Ling[a,b,d], Qiang Zhu[b,d], Magdalini Polymenidou[b,d,2], Kevin Drenner[a,b], Jonathan W. Artates[b,d], Melissa McAlonis-Downes[b,d], Sebastian Markmiller[d], Kasey R. Hutt[d], Donald P. Pizzo[e], Janet Cady[f], Matthew B. Harms[f], Robert H. Baloh[g], Scott R. Vandenberg[e], Gene W. Yeo[d], Xiang-Dong Fu[d], C. Frank Bennett[c], Don W. Cleveland[a,b,d,3], and John Ravits[a,3]

Departments of [a]Neurosciences, [d]Cellular and Molecular Medicine, and [e]Pathology, and [b]Ludwig Institute for Cancer Research, University of California, San Diego, La Jolla, CA 92093; [c]Isis Pharmaceuticals, Carlsbad, CA 92010; [g]Department of Neurology, Cedars-Sinai Medical Center, Los Angeles, CA 90048; and [f]Department of Neurology, Washington University School of Medicine, St. Louis, MO 63110

Contributed by Don W. Cleveland, October 7, 2013 (sent for review September 22, 2013)

Expanded hexanucleotide repeats in the chromosome 9 open reading frame 72 (*C9orf72*) gene are the most common genetic cause of ALS and frontotemporal degeneration (FTD). Here, we identify nuclear RNA foci containing the hexanucleotide expansion (GGGGCC) in patient cells, including white blood cells, fibroblasts, glia, and multiple neuronal cell types (spinal motor, cortical, hippocampal, and cerebellar neurons). RNA foci are not present in sporadic ALS, familial ALS/FTD caused by other mutations (*SOD1*, *TDP-43*, or *tau*), Parkinson disease, or nonneurological controls. Antisense oligonucleotides (ASOs) are identified that reduce GGGGCC-containing nuclear foci without altering overall *C9orf72* RNA levels. By contrast, siRNAs fail to reduce nuclear RNA foci despite marked reduction in overall *C9orf72* RNAs. Sustained ASO-mediated lowering of *C9orf72* RNAs throughout the CNS of mice is demonstrated to be well tolerated, producing no behavioral or pathological features characteristic of ALS/FTD and only limited RNA expression alterations. Genome-wide RNA profiling identifies an RNA signature in fibroblasts from patients with *C9orf72* expansion. ASOs targeting sense strand repeat-containing RNAs do not correct this signature, a failure that may be explained, at least in part, by discovery of abundant RNA foci with *C9orf72* repeats transcribed in the antisense (GGCCCC) direction, which are not affected by sense strand-targeting ASOs. Taken together, these findings support a therapeutic approach by ASO administration to reduce hexanucleotide repeat-containing RNAs and raise the potential importance of targeting expanded RNAs transcribed in both directions.

Expanded hexanucleotide repeats in the first intron of the chromosome 9 open reading frame 72 (*C9orf72*) gene were recently identified (1, 2) as the most common genetic cause of ALS, frontotemporal degeneration (FTD), or concomitant ALS/FTD (3, 4). The mechanisms by which the expanded repeats cause neurodegeneration are unknown, but leading candidate mechanisms are RNA-mediated toxicity, loss of the *C9orf72* gene function (from reduced *C9orf72* produced by the allele with the expansion), or a combination of the two.

RNA-mediated toxicity from nucleotide repeat expansion was initially described for CUG expansion in the RNA encoded by the *DMPK* gene in myotonic muscular dystrophy (5). A consensus view is that RNA toxicity plays a crucial role in a variety of repeat expansion disorders (6). A hallmark of these disorders is the accumulation of expanded transcripts into nuclear RNA foci (7). RNAs harboring a long stretch of repeats are thought to fold into stable structures and sequester RNA binding proteins, which, in turn, sets off a molecular cascade leading to neurodegeneration (7). In myotonic dystrophy, sequestration and functional disruption of the muscleblind-like family of RNA binding proteins are associated with specific splicing and expression changes in affected tissues (5, 8–12).

Sequestration of one or more RNA binding proteins into pathological RNA foci has also been proposed in ALS/FTD linked to *C9orf72* expansion (1, 13–16). It is anticipated, but has not been demonstrated, that sequestration of RNA binding proteins into expanded GGGGCC RNA foci may lead to major RNA processing alterations as in myotonic dystrophy. An alternative RNA-mediated toxicity mechanism to RNA binding protein sequestration is an unconventional repeat-associated non-ATG (RAN)–dependent translation that produces aberrant peptide or dipeptide polymers (17, 18). This mechanism was initially described in spinal cerebellar ataxia 8 (SCA8) and myotonic dystrophy type 1 (17), and polymeric dipeptides trans-

Significance

The most frequent genetic cause of ALS and frontotemporal degeneration is a hexanucleotide expansion in a noncoding region of the *C9orf72* gene. Similar to other repeat expansion diseases, we characterize the hallmark feature of repeat expansion RNA-mediated toxicity: nuclear RNA foci. Remarkably, two distinct sets of foci are found, one containing RNAs transcribed in the sense direction and the other containing antisense RNAs. Antisense oligonucleotides (ASOs) are developed that selectively target sense strand repeat-containing RNAs and reduce sense-oriented foci without affecting overall *C9orf72* expression. Importantly, reducing *C9orf72* expression does not cause behavioral or pathological changes in mice and induces only a few genome-wide mRNA alterations. These findings establish ASO-mediated degradation of repeat-containing RNAs as a significant therapeutic approach.

Author contributions: C.L.-T., M.B., F.R., S.S., A.T.W., M.P., X.-D.F., C.F.B., D.W.C., and J.R. designed research; C.L.-T., M.B., F.R., S.S., H.-R.L., J.J., A.T.W., S.C., M.K., J.Q., S.-C.L., Q.Z., M.P., K.D., J.W.A., M.M.-D., S.M., and J.C. performed research; F.R., H.-R.L., A.T.W., J.Q., M.B.H., R.H.B., S.R.V., G.W.Y., X.-D.F., C.F.B., and J.R. contributed new reagents/analytic tools; C.L.-T., M.B., F.R., S.S., P.L., H.-R.L., J.J., A.T.W., J.Q., Y.S., K.R.H., D.P.P., G.W.Y., D.W.C., and J.R. analyzed data; and C.L.-T., M.B., P.L., C.F.B., D.W.C., and J.R. wrote the paper.

The authors declare no conflict of interest.

Data deposition: The sequencing data from RNA-seq and MASP have been deposited in the Gene Expression Omnibus (GEO) database, http://www.ncbi.nlm.nih.gov/geo/.

[1]C.L.-T. and M.B. contributed equally to this work.

[2]Present address: Institute of Molecular Life Sciences, University of Zurich, CH-8057 Zurich, Switzerland.

[3]To whom correspondence may be addressed. E-mail: dcleveland@ucsd.edu or jravits@ucsd.edu.

This article contains supporting information online at www.pnas.org/lookup/suppl/doi:10.1073/pnas.1318835110/-/DCSupplemental.

lated from GGGGCC repeat-containing RNAs have been identified in tissues from *C9orf72* patients (19, 20).

A contribution of loss of *C9orf72* gene function to disease mechanism is supported in patients with expansions by reported reductions of *C9orf72* transcript levels (1, 2, 21) that may be triggered by expansion-driven hypermethylation at the *C9orf72* locus (22). The contribution of this reduction to neuronal death is not established, although loss of *C9orf72* during embryonic development is associated with motor deficits in zebrafish (23).

Irrespective of the relative contribution to neurodegeneration of either RNA-mediated toxicity mechanism, a therapy reducing expanded RNA transcripts will target both RNA binding protein sequestration and RAN translation. One means to achieve this is through use of antisense oligonucleotides (ASOs), which are short, single-stranded oligonucleotides that can be designed to hybridize to specific RNAs and modulate gene expression through a variety of mechanisms (24). The most prominent mechanism is DNA/RNA heteroduplex-induced cleavage by endogenous RNase H, which is a predominantly nuclear enzyme present in most mammalian cells; thus, RNA transcript reduction by this enzyme targets nuclear RNAs (24–26). ASOs infused into the nervous system have already gone to clinical trial for ALS caused by mutations in superoxide dismutase (SOD1) (27, 28) and are now being planned to go to trial for myotonic dystrophy (29) and Huntington disease (30). Further, using a strategy that modulates exon splicing rather than RNase H-mediated transcript reduction, ASOs are in clinical trial for spinal muscular atrophy (31–33).

Here, we identify that RNAs carrying expanded hexanucleotide repeats accumulate into foci in multiple cell types in the nervous systems of *C9orf72* patients with ALS/FTD. Further, we demonstrate the efficacy and tolerability of a therapeutic approach using ASOs against *C9orf72* RNAs to reduce the accumulation of expanded RNA foci selectively, even without affecting the overall level of *C9orf72*-encoding mRNAs. A genome-wide analysis is used to define an RNA profile linked to *C9orf72* expansion in patient fibroblasts. This genomic profile was not corrected by treatment with ASOs that reduce transcripts produced from the sense strand of the *C9orf72* gene. This result may be explained, at least in part, by identification of abundant GGCCCC repeat-containing RNA foci transcribed in the antisense direction from the *C9orf72* gene, which are not targeted by sense strand ASOs. All together, these results are consistent with a central role of RNA-mediated toxicity in the mechanism of neurodegeneration linked to *C9orf72* and provide crucial evidence supporting the therapeutic potential of ASOs in ALS and FTD.

Results

GGGGCC Expanded RNAs Accumulate into Foci in Peripheral Cells from *C9orf72* Patients. Skin biopsy-derived fibroblasts and immortalized lymphoblasts from *C9orf72* expansion-carrier patients

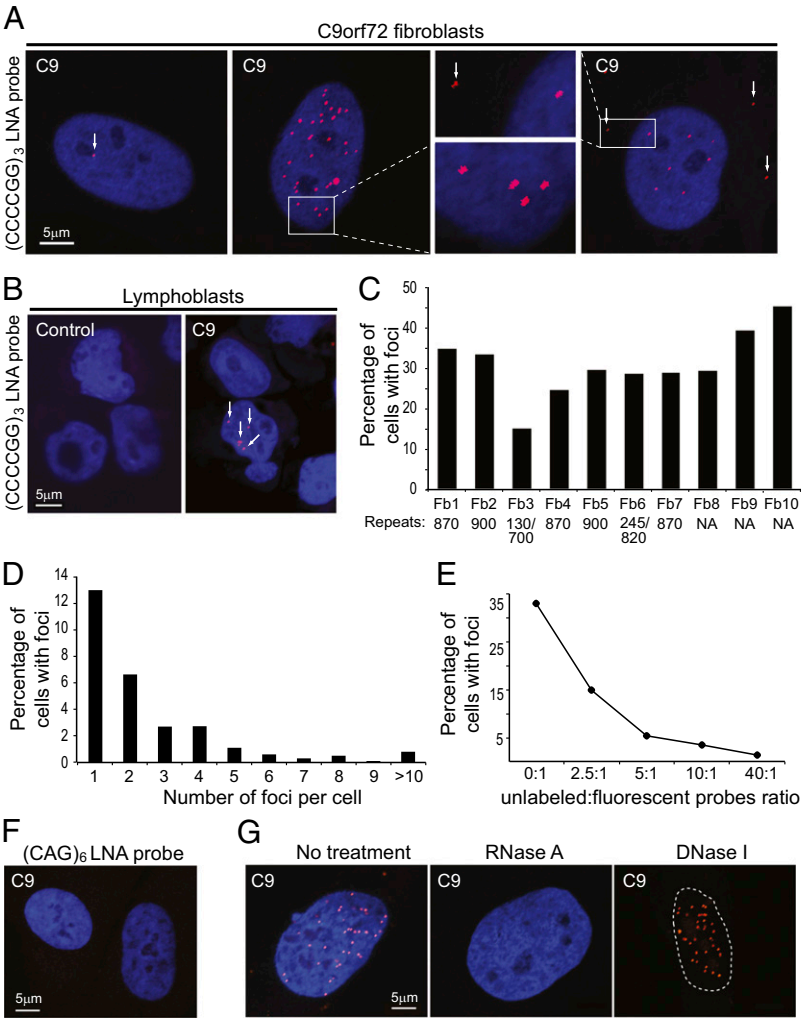

Fig. 1. Expanded GGGGCC RNA foci accumulate in peripheral cells from *C9orf72* patients. FISH was performed with a $(CCCCGG)_3$ LNA probe applied to fibroblasts (*A*) or lymphoblasts (*B*) from patients carrying GGGGCC repeat expansions in *C9orf72*. (*Left*) Arrow in *A* points to a single focus detected in the nucleus of one cell. (*Right*) Arrows in *A* (and the accompanying *Inset*) point to cytoplasmic foci found in rare cells. Arrows in *B* and left panel of *A* point to intranuclear foci. (*C*) Quantitation of the percentage of fibroblast cells with foci detected with the LNA probe as in *A*. Fibroblasts from patients with *C9orf72* expansion are denoted Fb-1 to Fb-10. The number of repeats estimated by DNA blot analysis (Fig. S2) is indicated for each fibroblast line. (*D*) Histogram shows the quantification of foci per nucleus in Fb-1. The specificity of the LNA probe for GGGGCC expansion-containing RNAs tested by competitive inhibition with a nonlabeled probe (*E*), use of an LNA probe complementary to a CTG repeat (*F*), and treatment with RNase A or DNase I (*G*) is shown. DNA is identified by staining with DAPI in *A*, *B*, *F*, and *G*.

with ALS were examined using FISH with locked nucleic acid (LNA) probes complementary to the GGGGCC hexanucleotide repeat. RNA foci of heterogeneous sizes (with dimensions between 0.2 and 0.5 μm) were identified in both cell types (Fig. 1 *A* and *B*). In the mitotically cycling fibroblasts, most foci were intranuclear, with occasional cytoplasmic foci, presumably due to previously intranuclear foci being excluded from reforming nuclei at mitotic exit (Fig. 1*A*, panels 3 and 4). Foci were present in fibroblasts from all nine patients with ALS tested carrying the *C9orf72* expansion, as well as in fibroblasts from a 62-y-old asymptomatic carrier of the hexanucleotide expansion [fibroblast-7 (Fb-7), *SI Appendix*, Table 1]. The size of the expansion determined by genomic DNA blotting varied between ∼130 and 900 repeats, with evidence for instability of the repeat in several fibroblast lines (Fig. 1*C* and Fig. S1). The fraction of cells containing foci varied between 15% and 45% in the cells from all 10 of these individuals (Fig. 1*C* and *SI Appendix*, Table 1). Foci were not observed in fibroblasts from 4 nonaffected individuals, four patients with sporadic ALS without a *C9orf72* expansion, four patients with ALS with a transactive response DNA-binding protein 43 (TDP-43) (N352S) mutation, and two patients with ALS due to SOD1 mutations (A4V or G41D) (Fig. S2 and *SI Appendix*, Table 1).

In 75% of instances, fibroblasts contained only one or two individual nuclear foci, but larger numbers [with up to 40 individual foci; Fig. 1 *A*, panel 2, and *D*] were also seen. Specificity of the signal obtained by in situ hybridization was supported by a competitive assay using coincubation with an unlabeled LNA probe, which revealed a dose-dependent competitive reduction of the number of cells containing foci (Fig. 1*E*), and by the lack of foci detected using LNA probes complementary to a CTG repeat (Fig. 1*F*). Most importantly, treatment with RNase A eliminated the foci, whereas treatment with DNase I eliminated chromosomal DNA (observed with DAPI) without affecting foci, evidence establishing that foci are composed primarily of RNA (Fig. 1*G*).

GGGGCC Expanded RNAs Accumulate into Foci in Neuronal and Glial Cells in Nervous Systems from Patients with *C9orf72* Repeat Expansions. The extent of hexanucleotide-containing RNA foci in tissues of the CNS was determined by FISH for 3 *C9orf72* ALS or ALS/FTD nervous systems and 25 nervous systems not carrying a *C9orf72* abnormal expansion (*SI Appendix*, Table 2). All analyses were performed by an observer blinded to the genotypes using autopsy samples acquired between 3 and 14 h postmortem from individuals between 21 and 84 y of age (*SI Appendix*, Table 2). Foci were identified in spinal motor neurons (identified by their large size and diffuse DAPI staining in the Rexed lamina IX of the anterior horn of the lumbar spinal cord) of all three nervous systems with *C9orf72* expansion (Fig. 2*A* and *SI Ap-*

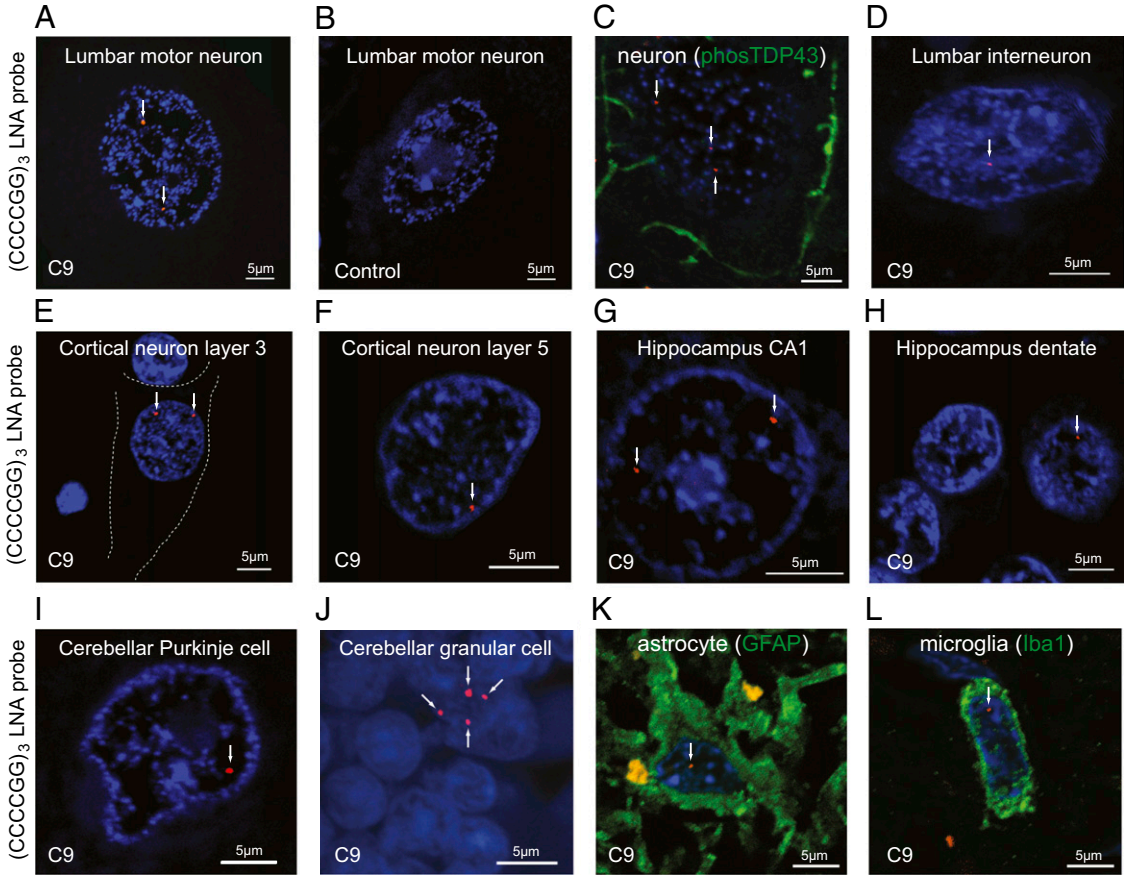

Fig. 2. GGGGCC-containing RNA foci accumulate in neurons and glial cells from *C9orf72* patients. FISH was performed with a $(CCCCGG)_3$ LNA probe applied to spinal cord or brain sections from patients carrying GGGGCC repeat expansions in *C9orf72* (*A* and *C*–*L*) or a nondisease control individual (*B*). DNA is stained with DAPI. Arrows point to intranuclear RNA foci. (*C*) FISH of a spinal motor neuron from a *C9orf72* expansion patient combined with indirect immunofluorescence with an antibody recognizing phosphorylated TDP-43 protein. FISH of a lumbar interneuron (*D*), layer 3 cortical neuron (*E*), layer 5 cortical neuron (*F*), hippocampal CA1 neuron (*G*), hippocampal dentate neurons (*H*), cerebellar Purkinje cell (*I*), or cerebellar granular cells (*J*) is shown. FISH of a spinal astrocyte or microglial cell from a *C9orf72* expansion patient combined with indirect immunofluorescence with antibodies recognizing GFAP (*K*) or Iba1 (*L*) is shown.

pendix, Table 2). No foci were identified in the nervous systems from 11 nonneurological control individuals, 11 patients with sporadic ALS, 1 patient with familial ALS with a *SOD1* mutation (A4V), 1 patient with Parkinson disease, and 1 sample from a patient carrying a mutation in *MAPT* (R5H) (Fig. 2*B*, Fig. S3, and *SI Appendix*, Table 2).

In all three nervous systems from patients with *C9orf72* expansion, clinical disease had begun in the bulbar region and advanced caudally. In two of these patients, there were moderate numbers of residual motor neurons in the lumbar area, and of these, ∼25–30% contained RNA foci. In the third nervous system, only a few motor neurons remained in the lumbar spinal cord, among which only 7% contained RNA foci. This is consistent with increased vulnerability of foci-containing cells during ALS degeneration. Most foci-containing motor neuron nuclei from all three *C9orf72* patients showed single inclusions, but nuclei with multiple foci were also identified (Fig. 2*A* and Fig. S3). Immunofluorescence staining with an antibody recognizing abnormal phospho–TDP-43 demonstrated that skeins of TDP-43-containing aggregates were not colocalized with the RNA foci in spinal motor neurons from *C9orf72* patients (Fig. 2*C*). A small proportion (2–4%) of nonmotor neuron cells (including interneurons in Rexed lamina VIII) in the lumbar region also contained nuclear foci (Fig. 2*D*).

In the brain, foci were identified in cortical, hippocampal, and cerebellar neurons. Foci were seen in about half of the pyramidal neurons in layers III and V of the motor cortex (Fig. 2 *E* and *F*). In the hippocampus, foci were present in about one-third to one-half of neurons in the dentate gyrus and CA1 neurons (Fig. 2 *G* and *H*). In the cerebellum, up to one-third of Purkinje cells contained foci (Fig. 2*I* and Fig. S4), although foci were found only rarely in cerebellar granule cells (Fig. 2*J*).

Importantly, using in situ hybridization coupled with fluorescent immunostaining to identify the corresponding cell type, RNA foci were found in a small proportion of astrocytes (identified by their expression of GFAP) (Fig. 2*K*) and in microglia [identified by expression of ionized calcium-binding adapter molecule 1 (Iba1), also known as allograft inflammatory factor 1 (AIF-1)] (Fig. 2*L*). Analysis of foci in oligodendrocytes was precluded by unresolved technical difficulties for coimmunofluorescence with oligodendrocyte markers and FISH.

ASOs, but Not siRNAs, Reduce Expanded GGGGCC RNA Foci. Recognizing that binding of single-stranded ASOs to a target RNA can induce cleavage of the RNA by endogenous, intranuclear RNase H (29, 34), we tested whether ASO-mediated RNA destruction could reduce intranuclear foci and if this could be successfully done without lowering overall *C9orf72* RNA levels. In designing ASOs, we exploited the presence of the pathogenic hexanucleotide expansion in an intron between two alternatively used first exons of the *C9orf72* gene. Transcription initiation at the two different sites leads to *C9orf72* pre-mRNAs that either contain the expansion or do not, with both encoding exactly the same polypeptide product (Fig. 3*A*). ASOs designed to bind upstream and downstream of the repeat were screened for effects on *C9orf72* transcripts in patient fibroblasts. Six ASOs targeting various regions of the *C9orf72* pre-mRNAs were selected for additional studies (Fig. 3*A* and *SI Appendix*, Table 3). Two, ASO-1 and ASO-2, hybridize to sequences within intron 1 upstream of the hexanucleotide expansion, and thereby exclusively target expansion-containing RNAs, whereas the remaining four ASOs (which hybridize to sequences in intron 1 downstream of exon 1b, exon 2, intron 5, and exon 11) were predicted to target all *C9orf72* RNA isoforms whether or not they contain the expansion. All ASOs contained 2′-O-(2-methoxyethyl) modifications to enhance stability and lower toxicity (24).

Within 24 h of introduction by transfection into fibroblasts, each of the six ASOs efficiently reduced the *C9orf72* repeat-containing RNA levels to 4–13% of the level in untreated

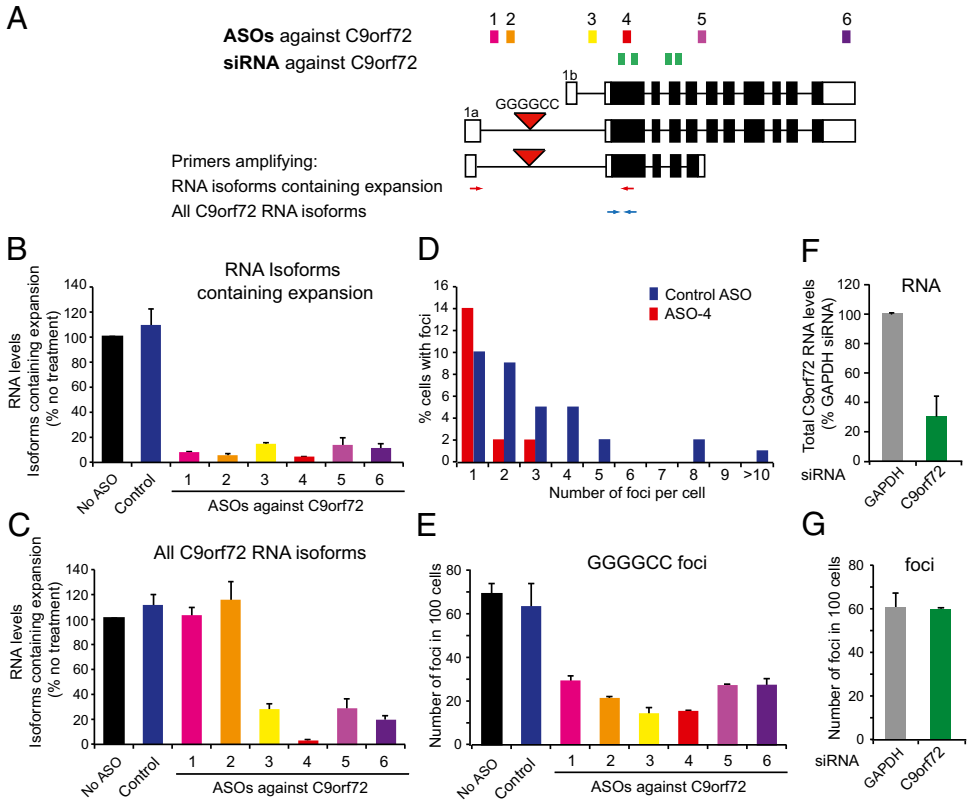

Fig. 3. ASOs complementary to *C9orf72* transcripts reduce GGGGCC nuclear foci. (*A*) Schematic drawing of the intron/exon structure of the *C9orf72* gene with its two transcription initiation sites and the GGGGCC hexanucleotide repeat in the first intron of RNAs initiated at the 5′-most transcription initiation site. (*Upper*) Positions of six ASOs and a pool of four siRNAs are shown. (*Lower*) Positions of primers for identifying the hexanucleotide containing RNA and all *C9orf72* RNAs are shown. Levels of RNAs containing the hexanucleotide repeat (*B*) or total *C9orf72* RNA isoforms (*C*), measured in total RNA isolated from Fb-1 24 h after no treatment (No ASO), transfection of a control ASO (targeting no human RNA), or each of the six *C9orf72*-targeting ASOs are shown. Percentage of cells with specific numbers of foci (*D*) or number of foci (per 100 cells) from cells transfected with ASOs (*E*), as in *B*, are shown. Levels of total *C9orf72* RNAs (*F*) or number of RNA foci in 100 cells (*G*) measured 24 h after transfection of Fb-1 cells with a pool of four siRNAs complementary to *C9orf72* RNA or control GAPDH siRNAs are shown. Error bars represent SE (SEM) from at least three independent experiments.

fibroblasts ($P < 0.0001$ for all ASOs compared with no treatment by t test) or in fibroblasts treated with a control ASO that did not have any target in the human genome (Fig. 3*B* and *SI Appendix*, Table 3). As expected, for the four ASOs targeting *C9orf72* RNA downstream of both alternative exons 1a and 1b, quantitative RT-PCR with primers amplifying all *C9orf72* RNA isoforms revealed that total *C9orf72* RNAs (including repeat-containing and repeat-lacking RNAs) were depleted [$P < 0.0001$ (by t test) for ASO-3, ASO-4, ASO-5, and ASO-6 compared with no treatment]. Strikingly however, ASO-1 and ASO-2, which target upstream of exon 1b, did not significantly reduce overall *C9orf72* RNA levels (Fig. 3*C*), despite efficient degradation of repeat-containing *C9orf72* RNAs (Fig. 3*B*). Thus, in human fibroblasts, the repeat-containing transcripts derived from the 5′ transcription initiation site are only a minor contributor to overall *C9orf72* RNA abundance.

FISH after ASO treatment was used to determine that all six ASOs significantly reduced the presence of RNA foci, regardless of the effect of the ASOs on the overall *C9orf72* transcript abundance (Fig. 3 *D* and *E*). All six of the *C9orf72* ASOs reduced the number of foci per cell, with a shift from cells initially accumulating more than 3 foci (including cells with more than 10 foci) to cells containing only 1–3 foci (Fig. 3*D*). Similarly, the average number of foci identified per 100 cells was reduced by two- to fivefold after treatment with ASOs targeting *C9orf72*, but not control ASOs ($P < 0.01$ for all ASOs compared with no treatment by t test; Fig. 3*E*). Remarkably, ASO-1 and ASO-2, which target pre-mRNA isoforms containing the GGGGCC repeat but do not reduce overall *C9orf72* RNA levels, were highly efficient in decreasing the number of foci (Fig. 3*E*).

An alternative approach for targeted RNA destruction is through the use of siRNAs that incorporate into the RNA-induced silencing complex (RISC) to mediate degradation of target RNAs (35, 36). As expected, when introduced by transfection, a pool of four different siRNAs targeting *C9orf72* exons 2 and 4 reduced *C9orf72* RNA levels to 30% of controls (Fig. 3*F* and *SI Appendix*, Table 3). However, despite this reduction, siRNA treatment did not affect accumulation of expanded RNA foci in fibroblasts from *C9orf72* patients (Fig. 3*G*), consistent with the preferential cytoplasmic location of the RISC complex (35, 37). Thus, in contrast to ASOs, siRNAs can efficiently provoke destruction of the normal, nonpathogenic *C9orf72* RNA species but do so without affecting the intranuclear retention of hexanucleotide-containing RNAs into foci.

***C9orf72* Depletion in the Adult Mouse CNS Is Well Tolerated.** We next tested the tolerability to *C9orf72* reduction throughout the CNS of adult mice. Three weeks after a single intracerebroventricular (ICV) stereotactic injection of a mouse-specific *C9orf72* ASO into the right lateral ventricle (Fig. 4*A* and *SI Appendix*, Table 3), reduction of *C9orf72* RNA levels was achieved to 30% and 40% of control levels in spinal cord and brain, respectively (Fig. 4 *B* and *C*; $P < 10^{-5}$ by t test in both brain and spinal cord at 3 wk after ASO treatment compared with saline treatment). Because ASO action within the rodent and primate nervous systems can be long-lived (30), sustained depletion of *C9orf72* RNA was observed as expected, with return only to ∼75% of the initial level even 18 wk after ASO injection (Fig. 4 *B* and *C*).

An antibody that recognizes the ASO's phosphorothioate backbone was used to determine its distribution within the CNS at 3, 6, 9, 12, and 18 wk postinjection. Similar to the distribution obtained by continuous ICV infusion of ASOs for 2 wk (30), a single ICV injection resulted in ASO accumulation throughout the CNS, including the cortex, hippocampus, and spinal cord (Fig. S5). The durable suppression of endogenous *C9orf72* RNAs achieved was accompanied by minimal neuroinflammation (as shown by the absence or small increase in Iba1/Aif1 mRNA expression in brain and spinal cord, respectively) (Fig. S6).

Abnormal aggregations of TDP-43, p62, and ubiquitin have been extensively described in the neuropathology of ALS and

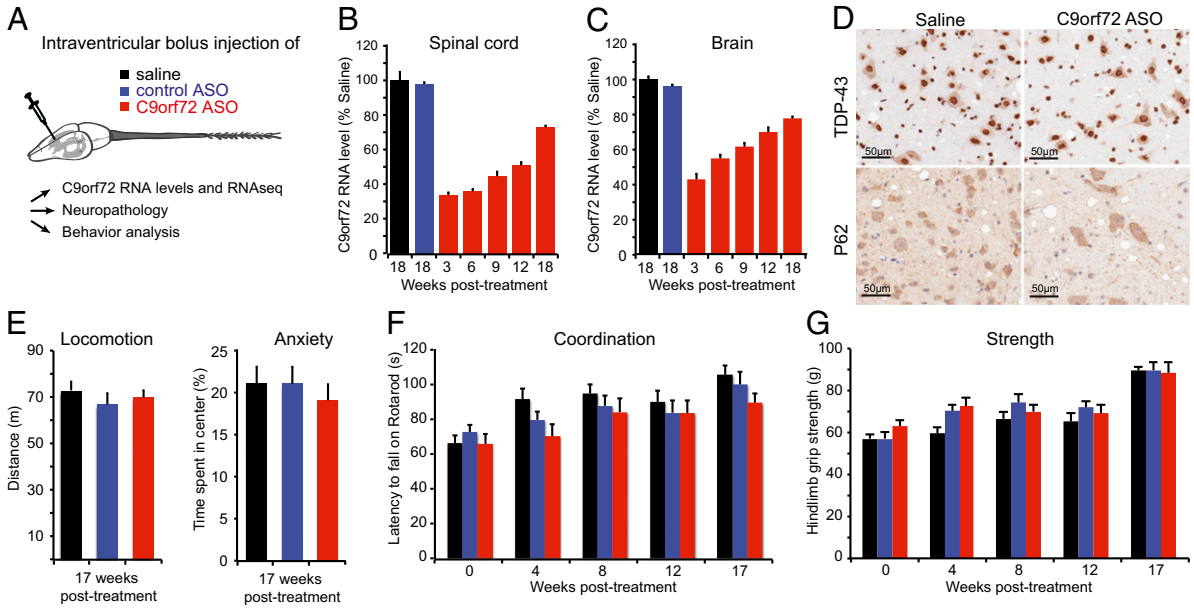

Fig. 4. Sustained depletion of *C9orf72* by ASO administration in the CNS does not trigger features of ALS/FTD. (*A*) Schematic of experimental design for bolus intraventricular injection of an ASO targeting *C9orf72* RNAs, control ASO, or saline, followed by determination of the level of *C9orf72* RNA reduction, neuropathological assessment, and determination of any phenotypic consequence. Levels of mouse *C9orf72* RNAs in spinal cord (*B*) and brain (*C*) were measured with quantitative RT-PCR at 3, 6, 9, 12, and 18 wk after ASO injection, as in *A*. (*D*) Immunohistochemistry to identify location of TDP-43 and p62 18 wk after intraventricular ASO infusion to lower *C9orf72* RNAs within the nervous systems of mice. (*E*–*G*) Assays of behavioral characteristics in mice following reduction in *C9orf72* RNAs induced by intraventricular ASO infusion. Error bars represent SE (SEM) from at least 5 biological replicates in B and *C* and 12 biological replicates in *E*–*G*.

FTD with *C9orf72* expansion (21, 38–40). After 18 wk of ASO-mediated depletion of *C9orf72* RNA, examination of tissue sections revealed that TDP-43 remained mainly nuclear in spinal cord, hippocampus, and cortex (Fig. 4*D*, *Upper*, and Fig. S7*A*). In addition, no p62 or ubiquitin aggregates were observed (Fig. 4*D*, *Lower*, and Fig. S7*B*), in contrast to the abnormal staining in an ALS mouse model carrying a $SOD1^{G85R}$ mutation (Fig. S7*B*).

To determine whether *C9orf72* depletion in the adult CNS triggered behavioral and/or motor deficits, a longitudinal assessment of strength, motor coordination, and anxiety was performed in mice after ICV injection of an ASO complementary to mouse *C9orf72* RNA or a control ASO ($n = 12$ per condition). Behavioral assays directed at measuring anxiety and ambient motor activity (open field) did not reveal any deficit in mice with *C9orf72* depletion (Fig. 4*E*). Similarly, no motor coordination or strength deficit was detected using rotarod and hind-limb grip strength assays at 4, 8, 12, and 17 wk after ASO injection (Fig. 4 *F* and *G*; $P > 0.24$ and $P > 0.12$ by t test at any time point for rotarod and grip strength, respectively, in animals treated with a *C9orf72* ASO vs. a control ASO).

Thus, long-term depletion of endogenous *C9orf72* RNAs to 30–40% of normal levels throughout the CNS did not trigger neuropathological or behavioral defects.

Few RNA Expression Changes in the Spinal Cord Follow Reduction of *C9orf72*. Following an approach that was used successfully to study the impact of TDP-43 or FUS/TLS loss in the CNS (41, 42), we used strand-specific, genome-wide sequencing of RNAs (43) to determine whether ASO-induced depletion of *C9orf72* provoked changes in RNA expression levels. Total RNA was extracted from spinal cords of mice 2 wk after stereotactic ICV injection of saline, an ASO complementary to mouse *C9orf72*, or a control ASO ($n = 3$ per condition) and converted to cDNA for high-throughput sequencing (43). For each sample, an average of 165 million non-redundant reads uniquely mapped to the mouse genome (version mm9) (*SI Appendix*, Table 4). Expression levels for each annotated protein-coding gene were determined by the number of mapped reads per kilobase of exon per million mapped reads (RPKM).

The sequence reads from three biological replicates treated with saline, *C9orf72* ASO, or a control oligonucleotide (*SI Appendix*, Table 4) were used to identify mRNAs encoded by 14,832 annotated protein-coding genes that satisfied the threshold of 0.5 RPKM in at least one condition. The RPKM ratio of the gene encoding *C9orf72* confirmed a reduction of *C9orf72* RNA to ~30% of normal levels (Fig. 5*A* and *SI Appendix*, Table 5). Statistical comparison of RPKM values between RNAs from *C9orf72* and control ASO-treated animals or *C9orf72*- and saline-treated samples revealed that only 12 genes were consistently up-regulated (defined by $P < 0.05$ adjusted for multiple testing) and 12 genes, including *C9orf72*, were down-regulated (defined by $P < 0.05$ adjusted for multiple testing) (Fig. 5*B* and *SI Appendix*, Table 5). Similar expression changes were observed in the different biological replicates (Fig. 5*B*), and expression levels after *C9orf72* depletion were confirmed for selected RNAs by quantitative RT-PCR of spinal cord RNA samples (Fig. 5*C*). Notably, only the mouse *C9orf72* gene (annotated *3110043O21Rik*) and the gene *Cyr61* encoding the cysteine-rich protein 61 were changed greater than twofold (*SI Appendix*, Table 5), a result contrasting greatly with the major expression changes involving several hundred genes observed after ASO-mediated depletion of TDP-43 or FUS/TLS (41, 42). The limited effect of *C9orf72* depletion on expression levels of other RNAs is consistent with the tolerability of *C9orf72* reduction in the adult CNS (Fig. 4).

Genome-Wide RNA Signature Can Be Defined in Fibroblasts with *C9orf72* Expansion. We next tested if *C9orf72* patient fibroblasts displayed major RNA expression alterations, as might be predicted if RNA foci disrupt function of one or more RNA binding protein(s). We exploited a streamlined genome-wide RNA sequencing strategy [multiplex analysis of polyA-linked sequences (MAPS)] recently developed to measure gene expression levels in a large number of samples (44). Expression profiling was performed on RNAs from fibroblasts of four *C9orf72* patients, four control individuals, and four patients with sporadic ALS (*SI Appendix*, Table 6). For each sample, an average of 11 million reads mapped to the human genome (version hg19) (*SI Appendix*, Table 6). Expression levels were determined by the number of mapped reads for each annotated protein-coding gene (44). Hierarchical clustering of expression values for all genes showed that the four *C9orf72* patient lines had an expression profile distinct from control and sporadic ALS lines. Three *C9orf72* patient lines (Fb-1, Fb-2, and Fb-3) clustered tightly together, with the fourth *C9orf72* patient line (Fb-4) revealing a less striking difference from the control fibroblasts (Fig. S8). Statistical comparison of expression values between the four *C9orf72* lines and the four control lines revealed that 122 genes were up-regulated [defined by a false discovery rate (FDR) <0.05] and 34 genes were down-regulated (defined by a FDR <0.05) in *C9orf72* patient fibroblasts (Fig. 5*D* and *SI Appendix*, Table 7).

We also determined the corresponding RNA profiles in *C9orf72* fibroblasts and control lines after reducing *C9orf72* RNA levels by transfection of a human *C9orf72* ASO (ASO-4; Fig. 3*A* and *SI Appendix*, Table 3). Despite reduction of *C9orf72* RNA levels to less than 10% of normal levels (Fig. 3*C*), only six expression changes accompanied ASO-mediated reduction of *C9orf72* in control fibroblasts (defined by a FDR <0.05; *SI Appendix*, Table 8), in agreement with our earlier observation that there is little change following suppression of *C9orf72* within the mouse nervous system (Fig. 5*B* and *SI Appendix*, Table 5). Importantly, *C9orf72* depletion in these control cells did not mimic the genome-wide RNA signature accompanying hexanucleotide expansion in *C9orf72* patient fibroblasts (Fig. 5*D* and *SI Appendix*, Table 7), providing evidence against a loss of *C9orf72* function as a cause of the disease-related RNA signature. ASO-mediated reduction of *C9orf72* RNA (*SI Appendix*, Table 7) efficiently reduced accumulation of GGGGCC RNA foci (Fig. 3 *D* and *E*). This did not, however, generate a reversal of the *C9orf72* RNA profile. Rather, hierarchical clustering (Fig. S8) showed that RNA profiles from each line continued to cluster together independent of the *C9orf72* expression level.

Antisense Strand of *C9orf72* Is Transcribed, and GGCCCC Expansions Accumulate into RNA Foci. Recognizing that in several other examples of expanded nucleotide repeat diseases, bidirectional transcription of the repeat has been identified (45–51), and that a recent study reported antisense transcripts in *C9orf72* patient nervous systems (20), we examined *C9orf72* patient fibroblasts for accumulation of RNAs transcribed in the antisense direction. Using FISH with LNA probes to the antisense strand of the hexanucleotide repeat GGCCCC, RNA foci were identified in all six fibroblasts from *C9orf72* expansion patients tested and were not observed in fibroblasts from three nonaffected individuals (Fig. 6*A*). Similar to sense strand foci, antisense strand foci had asymmetrical shapes with ~0.2- to 0.5-μm dimensions. Most were intranuclear, but an occasional cytoplasmic focus was identified.

As with sense strand foci, most fibroblasts from *C9orf72* patients contained a single antisense RNA-containing nuclear focus (Fig. 6*A*, *Left*), but multiple foci were also observed, with up to 90 individual fluorescent aggregates in the nucleus of a few affected cells (Fig. 6*B*). Indeed, antisense strand foci appeared more numerous than sense strand foci, although we note that no method exists to determine the relative sensitivities of the sense and antisense detection methods. Treatment with RNase A, but not with DNase I, eliminated the antisense strand foci, demonstrating that like their sense strand counterparts, they too were

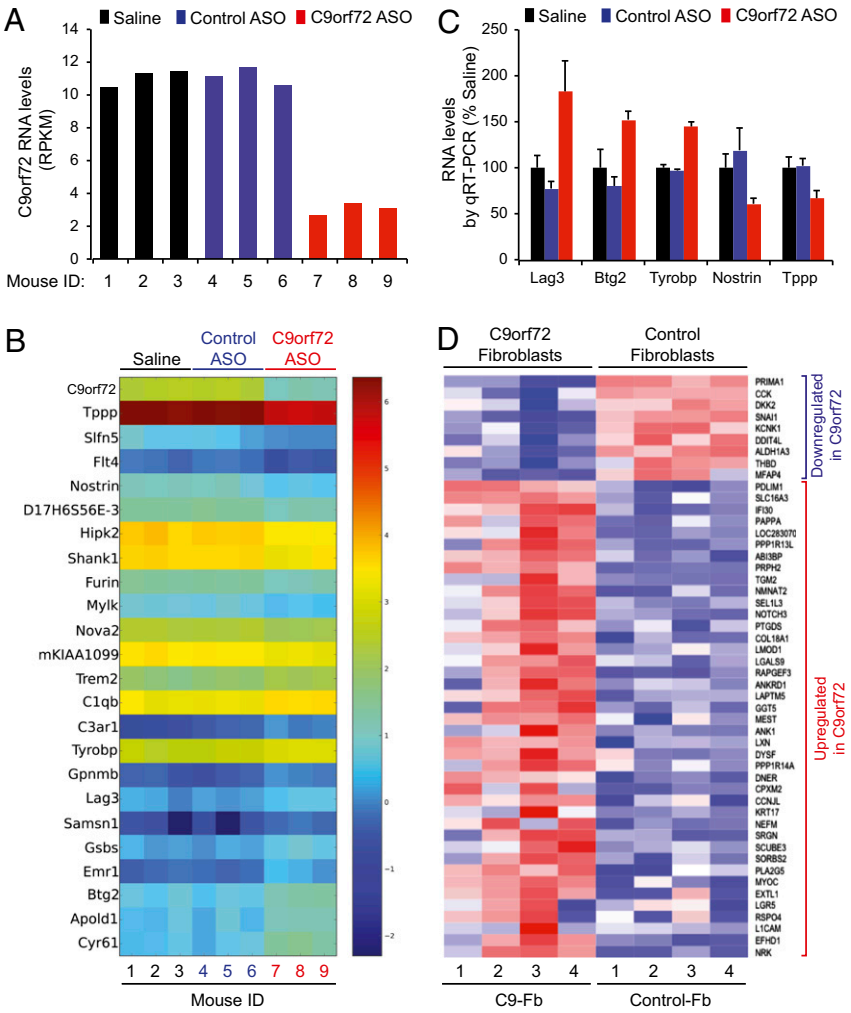

Fig. 5. RNA profiling in mouse spinal cord and in patient fibroblasts after ASO-mediated depletion of *C9orf72* RNAs. (*A*) Quantification of *C9orf72* RNA levels by strand-specific RNA sequencing in spinal cords from mice 2 wk after ICV administration of saline, a control ASO, or an ASO complementary to mouse *C9orf72*. RNA expression levels were determined by RPKM values. (*B*) Genome-wide identification in triplicate biological replicates of the 24 RNAs most affected in spinal cords from mice following intraventricular injection of an ASO to *C9orf72* RNA, a control ASO, or saline. (*C*) RNA levels determined for selected RNAs from *B*, measured by quantitative RT-PCR (qRT-PCR) after ASO-mediated depletion of *C9orf72* in mouse spinal cord. Error bars represent SE (SEM) from at least three biological replicates. (*D*) Heat map shows the top 50 genes from an RNA signature identified in fibroblasts of *C9orf72* patients vs. normal individuals, determined by genome-wide RNA profiling to identify RNAs down-regulated or up-regulated in *C9orf72* patient fibroblasts.

composed primarily of RNA (Fig. 6*B*). Antisense strand foci were also identified in neuronal and nonneuronal cells in the CNS of *C9orf72* patients (Fig. 6 *C–E*).

Importantly, treatment with ASOs that reduce sense strand-containing foci did not reduce the frequency of antisense strand foci (Fig. 6*F*), indicating that antisense transcription foci are independent of sense strand-containing foci. The failure to correct the RNA signature in *C9orf72* patient fibroblasts after treatment with ASOs targeting only sense strand repeat-containing RNAs (Fig. S8) may be explained by the unaltered accumulation of antisense RNA foci (Fig. 6*F*) potentially disrupting the function of RNA binding protein(s).

Discussion

ALS and FTD from repeat expansions in *C9orf72* belong to the TDP-43 proteinopathy spectrum of diseases, a group of disorders that include most instances of ALS and about 50% of patients with FTD, which are characterized by abnormal distribution of TDP-43 into cytoplasmic or intranuclear inclusions (52–54). Among these, ALS and FTD from repeat expansions in *C9orf72* display a unique neuropathology signature, including aggregation of protein biomarkers, such as p62, that are deposited in cerebellar Purkinje and granule cells and in hippocampal neurons (38, 39). To this specific signature, we now add the presence of nuclear RNA foci containing the hexanucleotide repeats transcribed from both sense and antisense strands.

RNA foci are the hallmark feature of repeat expansion disorders in which RNA-mediated toxicity is the principal pathogenic mechanism, including myotonic dystrophy types 1 and 2; fragile X and tremor and ataxia syndrome (FXTAS); SCA 3, SCA8, and SCA12; and Huntington disease-like 2 (6, 7). Foci had been originally reported in one patient with repeat expanded *C9orf72* ALS/FTD (1). We now demonstrate that sense strand RNA-containing foci are present in spinal motor neurons; smaller neurons deeper in the anterior horn; cerebellar Purkinje cells; cerebellar granule cells; hippocampal neurons; and pyramidal cells in the motor cortex, including layers III and V (Fig. 2). Similar RNA foci are also found in nonneuronal cells, including astrocytes and microglia, as well as in circulating white blood cells and primary fibroblasts (Figs. 1 and 2).

Our additional discovery of foci corresponding to antisense RNAs transcribed across the expanded repeat in the *C9orf72*

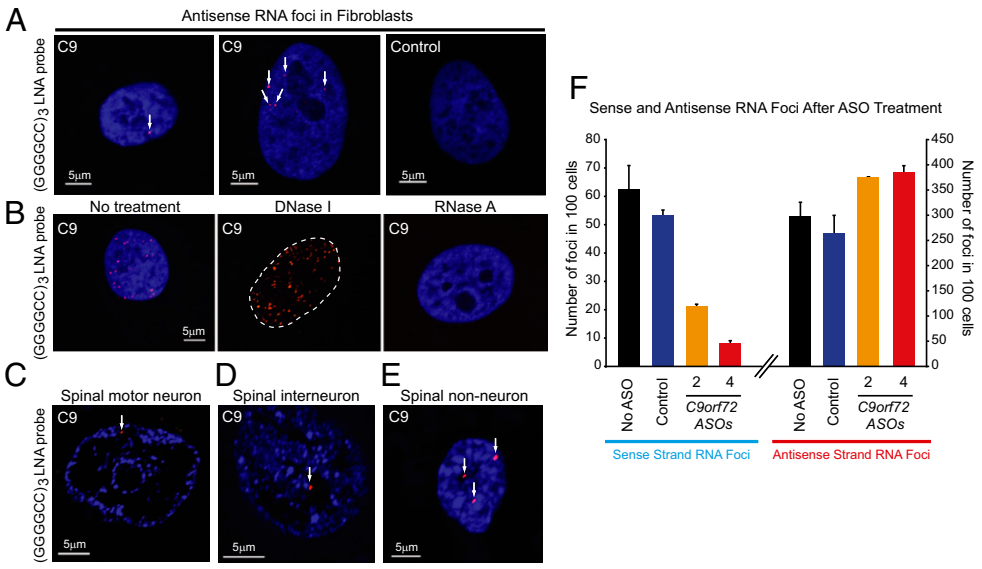

Fig. 6. GGCCCC-containing RNA foci transcribed from the antisense strand of *C9orf72* accumulate in cells from *C9orf72* patients. FISH was performed with a $(GGGGCC)_3$ LNA probe hybridized to fibroblasts from either of two patients with hexanucleotide expansion in *C9orf72* or a nondisease control individual (*A*), or from a spinal motor neuron (*C*), interneuron (*D*), or nonneuronal cell (*E*) in spinal cord sections from *a C9orf72* patient. Arrows in *A* (*Left* and *Center*) and in *C*–*E* point to foci. (*B*) Specificity of the $(GGGGCC)_3$ LNA probe determined by no treatment (*Left*), DNase I treatment (*Center*), or RNase A treatment (*Right*). (*F*) Numbers of sense and antisense strand repeat-containing RNAs detected by FISH in fibroblasts from a *C9orf72* expansion patient (Fb-5) 24 h following transfection of sense strand-targeting ASOs (ASO-2 or ASO-4). Error bars represent SE (SEM) from three independent experiments.

gene complements an initial report of the presence of antisense strand RNAs (20). Remarkably, our evidence has revealed that antisense foci seem more numerous than the sense strand foci and largely independent of them. Recent biochemical studies of in vitro constructs have shown that sense strand $r(GGGGCC)_n$, but not the antisense strand $r(GGCCCC)_n$, repeats form structures called G-quadruplexes, which have been proposed to affect cell functions, including genetic instability, telomere regulation, gene regulation, splicing, and RNA translation regulation (15, 55).

Although in most repeat expansion diseases, the sense strand transcript or its translated protein products are thought to have primacy in disease pathogenesis, discovery of antisense strand transcripts is leading to increasing appreciation of their potential significance in disease pathogenesis (45–51, 56). In FXTAS, antisense strand transcripts, as well as sense strand transcripts, are up-regulated, polyadenylated at the 3′ end, and capped at the 5′ end (47), although only the sense strand is known to generate nuclear inclusions (57). In none of these prior examples, however, have sense and antisense strands been found to generate nuclear foci concurrently.

Our finding of nuclear foci generated from both strands stands unique among the group of diseases mediated by RNA gain of function. Not yet determined is whether antisense strand RNAs that can be incorporated into antisense foci can also be translated into RAN polydipeptides, as has been shown for the sense strand (19, 20). Interestingly, poly-(glycine-proline), the polydipeptide most strongly demonstrated to accumulate in patient tissues by Ash et al. (19), is the only one of the five possible polydipeptides that is encoded by both sense and antisense strands. Regardless, the presence of sense and antisense RNA foci and our demonstration of an RNA signature linked to *C9orf72* repeat expansion that does not reflect the very modest RNA changes that accompany *C9orf72* loss of function offer strong support that RNA-mediated toxicity is a critical mechanism in the pathogenesis of ALS and FTD caused by repeat expansions.

Whether this RNA-mediated toxicity is related to sequestration of RNA binding proteins (13–16), to non-ATG (RAN) translation (18–20), or to both, ASOs that target degradation of the hexanucleotide-containing RNAs will act directly on the molecular species responsible for driving at least a central part of the disease mechanism. Indeed, we have identified here ASOs that selectively reduce accumulation of GGGGCC sense strand hexanucleotide-containing RNA foci, without significantly affecting the overall level of RNAs encoding the *C9orf72* polypeptide (Fig. 3), thereby enabling a therapeutic approach using ASOs to reduce the pathogenic, expansion-containing RNAs without inducing *C9orf72* protein loss. This selective targeting is in contrast to what happens with targeted RNA degradation through use of siRNAs. This latter approach reduces the nonpathogenic *C9orf72* RNA without affecting nuclear RNA foci, consistent with the primary site of action of siRNA within the cytoplasm.

Disease mechanisms in *C9orf72* repeat expanded ALS/FTD may include contributions from loss of *C9orf72* protein function. Although nothing is known about *C9orf72* function (58, 59), reduced levels of *C9orf72* RNAs have been reported in tissue samples from patients with *C9orf72* expansions (1, 2, 21). One potential issue with ASO-mediated reduction of *C9orf72* RNAs could be exacerbating the loss of *C9orf72* function. This possibility is mitigated by our demonstration that RNAs containing the hexanucleotide expansion can be selectively reduced without significant reduction in overall *C9orf72* RNA levels. Moreover, even for ASOs that target both repeat- and non–repeat-containing *C9orf72* RNAs, we have demonstrated that reducing *C9orf72* broadly within the rodent nervous system for several months does not produce a behavioral phenotype or neuropathological abnormalities (Fig. 4). This evidence supports that the abnormal accumulation of TDP-43, p62, and ubiquitin seen in patients with ALS and FTD with *C9orf72* expansions (21, 38–40) is not induced by a loss of *C9orf72* function mRNA and supports that ASO-mediated *C9orf72* reductions should be tolerated in an adult nervous system and may be safe to use in ALS and FTD.

Finally, although genome-wide RNA profiling identified an RNA signature in *C9orf72* patient fibroblasts (Fig. 5), ASOs targeting only sense strand repeat-containing RNAs did not

correct this RNA profile. This failure may be explained, at least in part, by RNA foci with *C9orf72* repeats transcribed in the antisense (GGCCCC) direction, which we have determined not to be affected by sense strand-targeting ASOs (Fig. 6). Of immediate interest now will be to determine the relative levels of sense and antisense transcripts in different cell types and tissues from controls and patients with *C9orf72* expansions. In addition, the development of ASOs targeting the antisense transcripts will undeniably represent a crucial step to evaluate the contribution of antisense expanded RNAs in disease pathogenesis. Indeed, taken together, our findings support that ASO therapy to reduce hexanucleotide repeat-containing RNAs is a rational and promising approach, but they also raise the important possibility that expanded RNAs transcribed from both directions may need to be targeted.

Methods

Fibroblasts, Lymphoblasts, and Human CNS Tissues. All human tissues were obtained and archived by way of an Institutional Review Board and Health Insurance Portability and Accountability Act-compliant Informed Consent process (Benaroya Research Institute, Seattle, WA IRB# 10058). Primary fibroblast cell lines were derived from patient skin biopsies, and immortalized lymphoblast lines were obtained from the Coriell Institute (ND11411 and ND12455). Primary fibroblasts were grown in high-glucose DMEM supplemented with 20% (vol/vol) tetracycline-free FBS, 2% (vol/vol) penicillin/streptomycin, and 1% amphotericin B. Immortalized lymphoblasts were proliferated in Iscove's modified Dulbecco's medium supplemented with 20% (vol/vol) tetracycline-free FBS and penicillin/streptomycin, and were attached to slides using a CytoSpin centrifuge (Thermo Scientific).

ALS nervous systems were obtained from patients who met the modified El Escorial criteria for definite ALS (60). Control nervous systems were obtained from nonneurological patients when life support was withdrawn or from patients on hospice. Autopsies were performed within 6 h of death, with an average postmortem interval of 4 h. Portions of the CNS were fixed in 10% neutral buffered formalin for more than 14 d, embedded in paraffin, and stored at room temperature.

Genotyping for *C9orf72* Expansion. Genotyping for the expanded GGGGCC repeat was performed by repeat-primed PCR as described elsewhere (2) using DNA extracted from patient cell lines or frozen brain or spinal cord tissues.

Southern Blot Quantification of *C9orf72* Expansion Size. Five micrograms of genomic DNA was isolated from patient-derived fibroblast cells and digested overnight with XbaI. Fragments were separated by electrophoresis at 35 V for 15 h on a 0.8% agarose gel and subsequently transferred to Amersham Hybond-N+ nylon membranes (GE Healthcare). A 590-bp probe was generated by PCR using the following primers: forward, AAATTGCGATGACTTTGCAGGGGACCGTGG and reverse, GCTCTCACAGTACTCGCTGAGGGTGAACAA. After gel purification, the probe was labeled with ^{32}P-dCTP (PerkinElmer) using the Random Primed DNA labeling kit (Life Technologies) and purified using Illustra ProbeQuant G-50 microcolumns (GE Healthcare). Hybridization was carried out overnight at 68 °C in Perfect Hyb Plus buffer (Sigma) containing 100 μg/mL salmon sperm DNA (Life Technologies). Membranes were washed twice for 5 min at room temperature with 2× SSC + 0.1% SDS and twice for 20 min at 68 °C with 0.2× SSC + 0.1% SDS. Amersham Hyperfilm ECL (GE Healthcare) was exposed with an intensifying screen at −80 °C for 5–10 d.

FISH. LNA (16-mer fluorescent)-incorporated DNA probes were used against the sense and antisense RNA hexanucleotide repeat (Exiqon, Inc.). The sequences of the probes are indicated in *SI Appendix*, Table 9. Probes of identical sequence were labeled with 5′ TYE-563 or nonfluorescent 5′/3′ digoxigenin (DIG). A 5′ TYE-563–labeled fluorescent probe targeting CAG repeats was used as a negative control. Exiqon batch numbers were 607323 (TYE-563) and 607565 (DIG) for the probes recognizing the sense strand hexanucleotide repeat, 610331 (TYE-563) and 611857 (DIG) for the probes recognizing the antisense strand hexanucleotide repeat, and 607324 for the probe recognizing CAG repeat, respectively.

Visualization of Foci. Primary visualization for quantification and imaging of foci was performed at 100× magnification using a Nikon Eclipse Ti confocal microscope system equipped with a Nikon CFI Apo TIRF 100× oil objective (N.A. = 1.49). Global quantification of spinal cord section nuclei was performed using image data obtained on a Hamamatsu Nanozoomer scanning microscope, and nuclei counts were made using the Threshold and Particle Counter commands in ImageJ64 (National Institutes of Health).

RNase-H–Mediated ASO Targeting of *C9orf72* RNA Transcripts in Primary Fibroblasts. ASOs designed and produced by Isis Pharmaceuticals (*SI Appendix*, Table 3) were transfected into primary human fibroblast lines. Patient or control fibroblast cells were plated into chamber slides 24 h before treatment. They were then washed in PBS and transfected using 1 μL/mL of Cytofectin Transfection Reagent (catalog no. T610001; Genlantis) and a final ASO concentration of 25 nM in OPTI-MEM (catalog no. 31985-070/088; Gibco). Cells were incubated 4 h in the presence of the transfection reagents. Twenty-four hours after transfection, the cells were fixed in 4% paraformaldehyde or were lysed for RNA extraction in buffer RLT (catalog no. 79216; Qiagen) or TRIzol reagent (catalog no. 15596-026; Life Technologies). Lysates were frozen immediately on dry ice, and fixed cells were immediately hybridized as described herein.

RNA Extraction and Quantitative RT-PCR from Human Fibroblasts. Total RNA extraction was done with an RNeasy 96 kit as instructed by the manufacturer (Qiagen). The RNA was reverse-transcribed and amplified using an Express One-Step SuperScript kit (Invitrogen). Quantitative RT-PCR reactions were conducted and analyzed on a StepOnePlus Real-Time PCR system (Applied Biosystems). The levels of human *C9orf72* transcripts were normalized to GAPDH, and the levels of ASO-treated fibroblasts were further normalized to the nontreated fibroblasts. Primers and probe sequences to amplify all isoforms of human *C9orf72* transcripts (located in exon 2) and to amplify only the isoforms containing exon 1a (located in exon 1a and exon 2) are indicated in *SI Appendix*, Table 9.

Injections of ASO in the Mouse CNS. All procedures were accomplished using a protocol approved by the Institutional Animal Care and Use Committee (Department of Health and Human Services, National Institutes of Health publication 86-23). To deplete *C9orf72* in vivo, ICV stereotactic injections of 10 μL of ASO solution, corresponding to a total of 500 μg of ASOs, were administered into the right ventricle of 8-wk-old female C57BL/6 mice using the following coordinates: 0.2 mm posterior and 1.0 mm lateral to the right from the bregma and 3 mm deep. Mice were monitored for any adverse effects until they were killed. Tissues collected for RNA analysis were a 1-mm coronal section of the brain located 2 mm posterior to the injection site and a 3-mm section of lumbar spinal cord.

At least 5 mice per condition [saline, a control ASO (catalog no. 456835; Isis Pharmaceuticals), or a mouse *C9orf72* ASO (catalog no. 571883; Isis Pharmaceuticals); *SI Appendix*, Table 3] and time points (3, 6, 9, and 12 wk postsurgery) were used to measure the duration of action of the mouse *C9orf72* ASO. Behavioral assays were performed after treating 12 mice per condition. The RNA-sequencing (RNA-seq) experiment was performed using 3 mice per condition with RNAs extracted from spinal cords dissected 2 wk after treatment.

Strand-Specific RNA-Seq Libraries. Strand-specific RNA-seq libraries were prepared from RNAs extracted from mouse spinal cords as described (41–43). RNA-seq libraries were sequenced on an Illumina Hi-Seq 2000 sequencer. The reads were aligned to a reference mouse genome obtained from the University of California, Santa Cruz (mm9, Build 37 from the National Center for Biotechnology Information and the Mouse Genome Consortium) using the spliced aligner Genomic Short-read Nucleotide Alignment Program (parameters were set to default, with the exception of reporting reads mapping to at most 10 places on the reference, –n 10). Gene expression was quantified using the read counts overlapping the gene position, normalizing to the gene in length (kilobases) and depth of sequencing (millions of reads). Statistical comparison of RPKM values between *C9orf72* and control ASO or *C9orf72* and saline-treated samples was performed with the DESeq software package (version 1.8.3) (Bioconductor).

MAPS Libraries. MAPS libraries were generated using RNA extracted with TRIzol (Invitrogen) from human fibroblasts as described elsewhere (44). Libraries were sequenced on an Illumina HiSeq-2000 sequencer using indexes for each sample for multiplexing of 12 samples per lane. Sequencing reads were mapped to the human genome (version hg19) using Bowtie software. The number of reads for each gene was determined, and the differential expression was analyzed using edgeR software (Bioconductor).

ACKNOWLEDGMENTS. We thank members of B. Ren's laboratory, especially Z. Ye, S. Kuan, and L. Edsall, for technical help with the Illumina sequencing; Kevin Clutario for technical assistance; all members of the D.W.C. laboratory for critical comments and suggestions on this project;

and the team at Isis Pharmaceuticals, especially Chris Hart, Sue Freier, and Gene Hung. C.L.-T. is the recipient of a Career Development Award from the Muscular Dystrophy Association. S.S. and Q.Z. are the recipients of Milton-Safenowitz postdoctoral fellowships from the Amyotrophic Lateral Sclerosis Association. S.-C.L. and J.J. are supported by National Institutes of Health Neuroplasticity of Aging Training Grant T32 AG 000216. M.P. was supported by a grant from the National Institutes of Health (Grant K99NS075216). This work was supported by research project funding from Target ALS to C.L.-T. (Grant 13-04827) and J.R. (Grant 13-44792), the Amyotrophic Lateral Sclerosis Association to J.R. (Grant 5356S3) and D.W.C. (Grant 2004), and the Packard Center for ALS Research at John Hopkins University (to D.W.C.). C.L.-T. and D.W.C. receive salary support from the Ludwig Institute for Cancer Research. J.R. receives salary support from University of California, San Diego.

1. DeJesus-Hernandez M, et al. (2011) Expanded GGGGCC hexanucleotide repeat in noncoding region of C9ORF72 causes chromosome 9p-linked FTD and ALS. *Neuron* 72(2):245–256.
2. Renton AE, et al.; ITALSGEN Consortium (2011) A hexanucleotide repeat expansion in C9ORF72 is the cause of chromosome 9p21-linked ALS-FTD. *Neuron* 72(2):257–268.
3. van Blitterswijk M, DeJesus-Hernandez M, Rademakers R (2012) How do C9ORF72 repeat expansions cause amyotrophic lateral sclerosis and frontotemporal dementia: Can we learn from other noncoding repeat expansion disorders? *Curr Opin Neurol* 25(6):689–700.
4. Ling SC, Polymenidou M, Cleveland DW (2013) Converging mechanisms in ALS and FTD: Disrupted RNA and protein homeostasis. *Neuron* 79(3):416–438.
5. Mankodi A, et al. (2000) Myotonic dystrophy in transgenic mice expressing an expanded CUG repeat. *Science* 289(5485):1769–1773.
6. Li LB, Bonini NM (2010) Roles of trinucleotide-repeat RNA in neurological disease and degeneration. *Trends Neurosci* 33(6):292–298.
7. Wojciechowska M, Krzyzosiak WJ (2011) Cellular toxicity of expanded RNA repeats: focus on RNA foci. *Hum Mol Genet* 20(19):3811–3821.
8. Charizanis K, et al. (2012) Muscleblind-like 2-mediated alternative splicing in the developing brain and dysregulation in myotonic dystrophy. *Neuron* 75(3):437–450.
9. Osborne RJ, et al. (2009) Transcriptional and post-transcriptional impact of toxic RNA in myotonic dystrophy. *Hum Mol Genet* 18(8):1471–1481.
10. Du H, et al. (2010) Aberrant alternative splicing and extracellular matrix gene expression in mouse models of myotonic dystrophy. *Nat Struct Mol Biol* 17(2):187–193.
11. Nakamori M, et al. (2013) Splicing biomarkers of disease severity in myotonic dystrophy. *Ann Neurol*, 10.1002/ana.23992.
12. Wang ET, et al. (2012) Transcriptome-wide regulation of pre-mRNA splicing and mRNA localization by muscleblind proteins. *Cell* 150(4):710–724.
13. Almeida S, et al. (2013) Modeling key pathological features of frontotemporal dementia with C9ORF72 repeat expansion in iPSC-derived human neurons. *Acta Neuropathol* 126(3):385–399.
14. Mori K, et al. (2013) hnRNP A3 binds to GGGGCC repeats and is a constituent of p62-positive/TDP43-negative inclusions in the hippocampus of patients with C9orf72 mutations. *Acta Neuropathol* 125(3):413–423.
15. Reddy K, Zamiri B, Stanley SY, Macgregor RB, Jr., Pearson CE (2013) The disease-associated r(GGGGCC)n repeat from the C9orf72 gene forms tract length-dependent uni- and multimolecular RNA G-quadruplex structures. *J Biol Chem* 288(14): 9860–9866.
16. Xu Z, et al. (2013) Expanded GGGGCC repeat RNA associated with amyotrophic lateral sclerosis and frontotemporal dementia causes neurodegeneration. *Proc Natl Acad Sci USA* 110(19):7778–7783.
17. Zu T, et al. (2011) Non-ATG-initiated translation directed by microsatellite expansions. *Proc Natl Acad Sci USA* 108(1):260–265.
18. Cleary JD, Ranum LP (2013) Repeat-associated non-ATG (RAN) translation in neurological disease. *Hum Mol Genet* 22(R1):R45–R51.
19. Ash PE, et al. (2013) Unconventional translation of C9ORF72 GGGGCC expansion generates insoluble polypeptides specific to c9FTD/ALS. *Neuron* 77(4):639–646.
20. Mori K, et al. (2013) The C9orf72 GGGGCC repeat is translated into aggregating dipeptide-repeat proteins in FTLD/ALS. *Science* 339(6124):1335–1338.
21. Gijselinck I, et al. (2012) A C9orf72 promoter repeat expansion in a Flanders-Belgian cohort with disorders of the frontotemporal lobar degeneration-amyotrophic lateral sclerosis spectrum: A gene identification study. *Lancet Neurol* 11(1):54–65.
22. Xi Z, et al. (2013) Hypermethylation of the CpG Island Near the G4C2 Repeat in ALS with a C9orf72 Expansion. *Am J Hum Genet*, 10.1016/j.ajhg.2013.04.017.
23. Ciura S, et al. (2013) Loss of function of C9orf72 causes motor deficits in a zebrafish model of Amyotrophic Lateral Sclerosis. *Ann Neurol*, 10.1002/ana.23946.
24. Bennett CF, Swayze EE (2010) RNA targeting therapeutics:Molecular mechanisms of antisense oligonucleotides as a therapeutic platform. *Annu Rev Pharmacol Toxicol* 50:259–293.
25. Crooke ST (1999) Molecular mechanisms of action of antisense drugs. *Biochim Biophys Acta* 1489(1):31–44.
26. Cerritelli SM, Crouch RJ (2009) Ribonuclease H: The enzymes in eukaryotes. *FEBS J* 276 (6):1494–1505.
27. Smith RA, et al. (2006) Antisense oligonucleotide therapy for neurodegenerative disease. *J Clin Invest* 116(8):2290–2296.
28. Miller TM, et al. (2013) An antisense oligonucleotide against SOD1 delivered intrathecally for patients with SOD1 familial amyotrophic lateral sclerosis: A phase 1, randomised, first-in-man study. *Lancet Neurol* 12(5):435–442.
29. Wheeler TM, et al. (2012) Targeting nuclear RNA for in vivo correction of myotonic dystrophy. *Nature* 488(7409):111–115.
30. Kordasiewicz HB, et al. (2012) Sustained therapeutic reversal of Huntington's disease by transient repression of huntingtin synthesis. *Neuron* 74(6):1031–1044.
31. Hua Y, et al. (2010) Antisense correction of SMN2 splicing in the CNS rescues necrosis in a type III SMA mouse model. *Genes Dev* 24(15):1634–1644.
32. Hua Y, et al. (2011) Peripheral SMN restoration is essential for long-term rescue of a severe spinal muscular atrophy mouse model. *Nature* 478(7367):123–126.
33. Rigo F, Hua Y, Krainer AR, Bennett CF (2012) Antisense-based therapy for the treatment of spinal muscular atrophy. *J Cell Biol* 199(1):21–25.
34. Condon TP, Bennett CF (1996) Altered mRNA splicing and inhibition of human E-selectin expression by an antisense oligonucleotide in human umbilical vein endothelial cells. *J Biol Chem* 271(48):30398–30403.
35. Carthew RW, Sontheimer EJ (2009) Origins and Mechanisms of miRNAs and siRNAs. *Cell* 136(4):642–655.
36. Mello CC, Conte D, Jr. (2004) Revealing the world of RNA interference. *Nature* 431 (7006):338–342.
37. Zeng Y, Cullen BR (2002) RNA interference in human cells is restricted to the cytoplasm. *RNA* 8(7):855–860.
38. Troakes C, et al. (2011) An MND/ALS phenotype associated with C9orf72 repeat expansion: Abundant p62-positive, TDP-43-negative inclusions in cerebral cortex, hippocampus and cerebellum but without associated cognitive decline. *Neuropathology* 32(5):505–514.
39. Al-Sarraj S, et al. (2011) p62 positive, TDP-43 negative, neuronal cytoplasmic and intranuclear inclusions in the cerebellum and hippocampus define the pathology of C9orf72-linked FTLD and MND/ALS. *Acta Neuropathol* 122(6):691–702.
40. Brettschneider J, et al. (2012) Pattern of ubiquilin pathology in ALS and FTLD indicates presence of C9ORF72 hexanucleotide expansion. *Acta Neuropathol* 123(6):825–839.
41. Polymenidou M, et al. (2011) Long pre-mRNA depletion and RNA missplicing contribute to neuronal vulnerability from loss of TDP-43. *Nat Neurosci* 14(4):459–468.
42. Lagier-Tourenne C, et al. (2012) Divergent roles of ALS-linked proteins FUS/TLS and TDP-43 intersect in processing long pre-mRNAs. *Nat Neurosci* 15(11):1488–1497.
43. Parkhomchuk D, et al. (2009) Transcriptome analysis by strand-specific sequencing of complementary DNA. *Nucleic Acids Res* 37(18):e123.
44. Fox-Walsh K, Davis-Turak J, Zhou Y, Li H, Fu XD (2011) A multiplex RNA-seq strategy to profile poly(A+) RNA: Application to analysis of transcription response and 3′ end formation. *Genomics* 98(4):266–271.
45. Cho DH, et al. (2005) Antisense transcription and heterochromatin at the DM1 CTG repeats are constrained by CTCF. *Mol Cell* 20(3):483–489.
46. Moseley ML, et al. (2006) Bidirectional expression of CUG and CAG expansion transcripts and intranuclear polyglutamine inclusions in spinocerebellar ataxia type 8. *Nat Genet* 38(7):758–769.
47. Ladd PD, et al. (2007) An antisense transcript spanning the CGG repeat region of FMR1 is upregulated in premutation carriers but silenced in full mutation individuals. *Hum Mol Genet* 16(24):3174–3187.
48. Chung DW, Rudnicki DD, Yu L, Margolis RL (2011) A natural antisense transcript at the Huntington's disease repeat locus regulates HTT expression. *Hum Mol Genet* 20(17): 3467–3477.
49. Sopher BL, et al. (2011) CTCF regulates ataxin-7 expression through promotion of a convergently transcribed, antisense noncoding RNA. *Neuron* 70(6):1071–1084.
50. Wilburn B, et al. (2011) An antisense CAG repeat transcript at JPH3 locus mediates expanded polyglutamine protein toxicity in Huntington's disease-like 2 mice. *Neuron* 70(3):427–440.
51. Batra R, Charizanis K, Swanson MS (2010) Partners in crime: Bidirectional transcription in unstable microsatellite disease. *Hum Mol Genet* 19(R1):R77–R82.
52. Neumann M, et al. (2006) Ubiquitinated TDP-43 in frontotemporal lobar degeneration and amyotrophic lateral sclerosis. *Science* 314(5796):130–133.
53. Lagier-Tourenne C, Cleveland DW (2009) Rethinking ALS: The FUS about TDP-43. *Cell* 136(6):1001–1004.
54. Lagier-Tourenne C, Polymenidou M, Cleveland DW (2010) TDP-43 and FUS/TLS: Emerging roles in RNA processing and neurodegeneration. *Hum Mol Genet* 19(R1): R46–R64.
55. Fratta P, et al. (2012) C9orf72 hexanucleotide repeat associated with amyotrophic lateral sclerosis and frontotemporal dementia forms RNA G-quadruplexes. *Sci Rep* 2:1016.
56. Pearson CE (2011) Repeat associated non-ATG translation initiation: One DNA, two transcripts, seven reading frames, potentially nine toxic entities! *PLoS Genet* 7(3): e1002018.
57. Tassone F, Iwahashi C, Hagerman PJ (2004) FMR1 RNA within the intranuclear inclusions of fragile X-associated tremor/ataxia syndrome (FXTAS). *RNA Biol* 1(2):103–105.
58. Levine TP, Daniels RD, Gatta AT, Wong LH, Hayes MJ (2013) The product of C9orf72, a gene strongly implicated in neurodegeneration, is structurally related to DENN Rab-GEFs. *Bioinformatics* 29(4):499–503.
59. Zhang D, Iyer LM, He F, Aravind L (2012) Discovery of Novel DENN Proteins: Implications for the Evolution of Eukaryotic Intracellular Membrane Structures and Human Disease. *Front Genet* 3:283.
60. Brooks, et al. (2000) El escorial revisited: revised criteria for the diagnosis of amyotrophic lateral sclerosis. *Amyotroph Lateral Scler Other Motor Neuron Disord* 1(5): 293–299.